Int. J. Heat Mass Transfer. Vol. 21, pp. 175–185. Pergamon Press 1978. Printed in Great Britain

THE EFFECT OF SUCTION AND SLIP VELOCITY OF A NON-NEWTONIAN FLUID FLOWING OVER A CIRCULAR CYLINDER

MARTIN SCHMAL and ANTONIO MACDOWEL FIGUEIREDO
COPPE/UFRJ, Programa de Engenharia Mecânica, 20000—Rio de Janeiro, Brazil

(*Received* 13 *October* 1975 *and in revised form* 21 *March* 1977)

Abstract—In this work the effect of suction and slip velocity for the forced convection of a Newtonian and a "power law" fluid flow on a circular cylinder is studied. The momentum and mechanical energy equations, the compatibility and suction conditions are derived and solved using a triparametric variable polynomial for the velocity profile The method of Geropp and Walz is used for the solution and the external velocity profile of Hiemez–Görtler was applied for the flow on a circular cylinder.

The suction effect can be well observed accompanying the wall shear stress and the suction parameter along the surface. Without suction the separation point of a non-Newtonian flow is anticipated when compared to a Newtonian flow on a circular cylinder. Applying suction the separation point was dislocated. The suction effect is more pronounced on the wall shear stress profile and mainly for the de-accelerated flow and higher suction levels. The suction parameter increases more rapidly in the neighbourhood of the separation point. The slip velocity effect is negligible.

NOMENCLATURE

x, y, coordinate system;
η, dimensionless, y/δ;
θ, angle;
δ, thickness;
δ_1, displacement thickness;
δ_2, momentum thickness;
δ_3, energy loss thickness;
L, length;
R, radius;
Z, thickness parameter;
u, tangential velocity;
v, normal velocity;
u_0, interface velocity;
p, pressure;
ρ, density;
μ, viscosity;
m, consistent index;
τ, shear stress;
g, gravity;
M_δ, local Mach number;
Re_∞, Reynolds number of potential flow;
Re_{δ_2}, local Reynolds number;
Fr, Froude number;
ψ_∞, suction number of the potential flow;
ψ_{δ_2}, local suction number;
∇, suction level;
c_f, drag coefficient;
C_D, dissipation coefficient;
β, integral of the dissipation coefficient;
ξ, variable exponent of the velocity profile;
a_i, coefficients of the velocity profile;
H_{32}, form parameter of the velocity profile;
Γ, form parameter of the velocity;
χ, suction parameter;
k, slip velocity parameter;
H_{12}, parameter of the velocity profile;
α, parameter of the velocity profile;
ε, parameter of the velocity profile;
γ, parameter of the velocity profile;
F, coefficient.

Index

i, iteration;
∞, external flow;
δ, at the edge of the boundary layer;
0, at the interface;
J, momentum quantities;
E, energy quantities;
S, separation point;
$*$, dimensionless.

INTRODUCTION

THE BEHAVIOUR of a non-Newtonian fluid flowing on surfaces was first considered by Acrivos, Shah and Petersen [1] applying the boundary-layer theory. They considered the power law model and, for the solution of the boundary-layer equations, the method due to von Kàrmàn–Pohlhausen was used. Bizzel and Slattery [2] used the same approach for the axisymmetric bidimensional power-law fluid flow. This case was extended by Neves [5] for the flow on a circular cylinder considering also a slip velocity on the surface.

Suction effect studies were considered only for Newtonian fluid. Spalding and Evans [9] presented a similar solution considering the effect of the suction parameter for the cone type flow. Truckenbrodt [10] studied the axisymmetric flow with suction using the integral method.

This work studies the effect of suction for the forced convection of a power law fluid flow on a circular cylinder considering the slip velocity at the surface. Integral equations are derived and a triparametric variable polynomial is used for the velocity profile.

THE BOUNDARY-LAYER EQUATIONS

Figure 1 illustrates the physical model and the coordinate system. The fluid flows by forced convection over a circular cylinder with suction applied along the surface. The pressure, viscous and the inertial forces are considered. The body forces can be neglected considering that the Froude number is greater than 2000 [7]. For larger Reynolds numbers

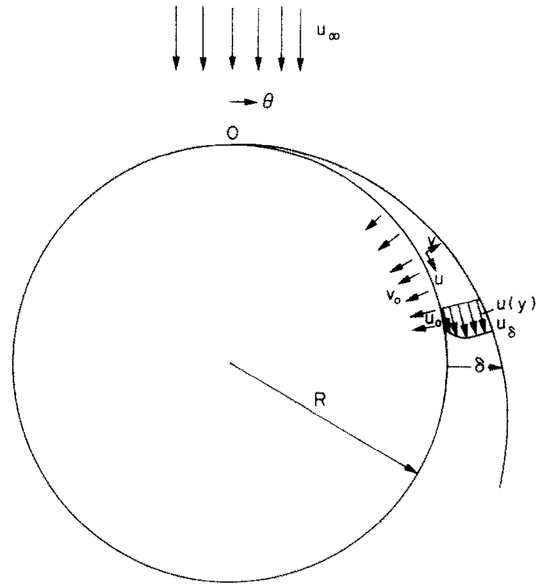

FIG. 1.

viscous effects are limited to a thin region near to the solid surface. The normal rate of momentum transport is more intensive than the tangential rate. Hence, the boundary-layer theory is applicable for the solution of this problem. Assuming laminar and steady-state flow and a power law model, the following boundary-layer equations are considered: continuity equation

$$\frac{\partial}{\partial x}(\rho u)+\frac{\partial}{\partial y}(\rho v)=0, \quad (1)$$

and motion equation

$$\rho\left(u\frac{\partial u}{\partial x}+v\frac{\partial u}{\partial y}\right)=-\frac{\mathrm{d}p}{\mathrm{d}x}+\frac{\partial \tau_{yx}}{\partial y} \quad (2)$$

where

$$\tau_{yx}=m\left(-\frac{\partial u}{\partial y}\right)^n \quad (3)$$

with the following boundary conditions, considering slip velocity and suction on the surface of the cylinder.

$$y=0 \qquad u=u_0(x) \quad (4)$$

$$v=v_0(x)$$

$$y=\delta \qquad u=u_\delta(x). \quad (5)$$

The integral equations

Applying the method of Wieghardt [11], the partial differential boundary-layer equations are transformed into ordinary differential equations by multiplying equations (1) and (2) by the weight functions $u^{\nu+1}/(\nu+1)$ and u^ν respectively. After some algebraic manipulations the following system of integral equation is obtained:

$$\frac{\mathrm{d}f_\nu}{\mathrm{d}x}+\left[(\nu+2)+\frac{g_\nu}{f_\nu}-M_\delta^2\right]f_\nu\frac{1}{u_\delta}\frac{\mathrm{d}u_\delta}{\mathrm{d}x}+e_\nu+h_\nu=0 \quad (6)$$

where

$$e_\nu=(\nu+1)\int_0^\delta\left(\frac{u}{u_\delta}\right)^\nu\frac{\partial}{\partial y}\left(\frac{\tau}{\rho_\delta u_\delta^2}\right)\mathrm{d}y, \quad (7)$$

$$f_\nu=\int_0^\delta\frac{\rho u}{\rho_\delta u_\delta}\left[1-\left(\frac{u}{u_\delta}\right)^{\nu+1}\right]\mathrm{d}y \quad (8)$$

$$g_\nu=(\nu+1)\int_0^\delta\frac{\rho u}{\rho_\delta u_\delta}\left[\frac{\rho_\delta}{\rho}\left(\frac{u}{u_\delta}\right)^{\nu-1}-1\right]\mathrm{d}y \quad (9)$$

and

$$h_\nu=\frac{\rho_0 v_0}{\rho_\delta u_\delta}(k^{\nu+1}-1) \quad (10)$$

with

$$k=\frac{u_0}{u_\delta}.$$

The slip velocity $u_0(x)$ is assumed to be proportional to the potential velocity $u_\delta(x)$. From equation (6) several ordinary differential equations or integral conditions are obtained. It is important to verify which values of ν have physical meaning satisfying the boundary conditions. Note that for $\nu=0$ the multiplying factor $(u/u_\delta)^\nu$ does not affect the boundary-layer equation. Otherwise, for $\nu=1$, the multiplying factor of the boundary-layer equation is equal to u/u_δ and less information can be drawn from the integral equations in the neighbourhood of the wall. For values of ν higher than one, less information is drawn from the integral conditions of equation (6). Finally for $\nu\to\infty\,(u/u_\delta=0)$ all characteristics of the boundary layer disappear, leaving, however, the trivial condition given by the continuity equation [11]. The values of $\nu=0$ and $\nu=1$ are particularly important for the solution of the system of equations (6), having a special well-known physical meaning.

The momentum and mechanical energy equations

For $\nu=0$, equations (7)–(10) result in:

$$e_0=\int_0^\delta\frac{\partial}{\partial y}\left(\frac{\tau}{\rho_\delta u_\delta^2}\right)\mathrm{d}y=-\frac{\tau_0}{\rho_\delta u_\delta^2}=-\frac{c_f}{2} \quad (11)$$

where c_f is the drag coefficient,

$$f_0=\int_0^\delta\frac{\rho u}{\rho_\delta u_\delta}\left(1-\frac{u}{u_\delta}\right)\mathrm{d}y=\delta_2 \quad (12)$$

where δ_2 is the momentum thickness,

$$g_0=\int_0^\delta\left(1-\frac{\rho u}{\rho_\delta u_\delta}\right)\mathrm{d}y=\delta_1 \quad (13)$$

where δ_1 is the displacement thickness, and

$$h_0\frac{\rho_0 v_0}{\rho_\delta u_\delta}\left(\frac{u_0}{u_\delta}-1\right). \quad (14)$$

Then substituting equations (11)–(14) in equation (6) results in the following momentum equation:

$$\frac{d\delta_2}{dx}+\left(2+\frac{\delta_1}{\delta_2}-M_\delta^2\right)\frac{\delta_2}{u_\delta}\frac{du_\delta}{dx}-\frac{c_f}{2}-(1-K)\frac{\rho_0 v_0}{\rho_\delta u_\delta}=0. \quad (15)$$

For $v = 1$ equations (7)–(10) results:

$$e_1 = 2\int_0^\delta \frac{u}{u_\delta}\frac{\partial}{\partial y}\left(\frac{\tau}{\rho_\delta u_\delta^2}\right)dy = -\frac{2}{\rho_\delta u_\delta^3}\left[u_0\tau_0+\int_{u_0}^{u_\delta}\tau\,du\right] = -2C_D \quad (16)$$

where C_D is the dissipation coefficient,

$$f_1 = \int_0^\delta \frac{\rho u}{\rho_\delta u_\delta}\left[1-\left(\frac{u}{u_\delta}\right)^2\right]dy = \delta_3 \quad (17)$$

where δ_3 is the energy loss thickness,

$$g_1 = 2\int_0^\delta \frac{\rho u}{\rho_\delta u_\delta}\left[\frac{\rho_\delta}{\rho}-1\right]dy = 2\delta_4 \quad (18)$$

where δ_4 is the density loss thickness and

$$h_1 = \frac{\rho_0 v_0}{\rho_\delta u_\delta}\left[\left(\frac{u_0}{u_\delta}\right)^2-1\right] = (k^2-1)\frac{\rho_0 v_0}{\rho_\delta u_\delta}. \quad (19)$$

Substituting the equations (17)–(19) in equation (6) results in the following mechanical energy equation

$$\frac{d\delta_3}{dx}+\left(3+2\frac{\delta_4}{\delta_3}-M_\delta^2\right)\frac{\delta_3}{u_\delta}\frac{du_\delta}{dx}-2C_D-(1-k^2)\frac{\rho_0 v_0}{\rho_\delta u_\delta}=0. \quad (20)$$

These equations are valid for steady-state, laminar flow with arbitrary pressure gradient, suction at the wall, slip velocity and variable physical properties.

For incompressible flow these equations are simplified, for

$$M_\delta = 0$$
$$\delta_4 = 0.$$

The compatibility condition

Applying the boundary condition for $y = 0$ to equation (2) reduces to:

$$\rho_0\left[u_0\frac{du_0}{dx}+v_0\left.\frac{\partial u}{\partial y}\right|_{y=0}\right] = \rho_\delta u_\delta\frac{du_\delta}{dx}+\left.\frac{\partial\tau}{\partial y}\right|_{y=0}$$

where ρ_0 is the density at the wall. Nothing that $u_0 = ku_\delta$, for k = const $du_0/dx = k(du_\delta/dx)$ it follows:

$$v_0\left.\frac{\partial u}{\partial y}\right|_{y=0}-\left(\frac{\rho_\delta}{\rho_0}-k^2\right)\frac{du_\delta}{dx} = \frac{1}{\rho_0}\left.\frac{\partial\tau}{\partial y}\right|_{y=0}.$$

Then for a power law fluid this equation is transformed to:

$$v_0\left.\frac{\partial u}{\partial y}\right|_{y=0}-\left(\frac{\rho\delta}{\rho_0}-k^2\right)\frac{du_\delta}{dx} = \frac{1}{\rho_0}\left[\frac{\partial m}{\partial y}\left(\frac{\partial u}{\partial y}\right)^n+nm\left(\frac{\partial u}{\partial y}\right)^{n-1}\frac{\partial^2 u}{\partial y^2}\right]_{y=0}. \quad (21)$$

Assuming incompressible flow, $\rho_0 = \rho_\delta = \rho$ and isothermic $(\partial m/\partial y = 0)$ results:

$$v_0\left.\frac{\partial u}{\partial y}\right|_{y=0}-(1-k^2)\frac{du_\delta}{dx} = n\frac{m}{\rho}\left[\left(\frac{\partial u}{\partial y}\right)^{n-1}\frac{\partial^2 u}{\partial y^2}\right]_{y=0}. \quad (22)$$

The Reynolds number for a power law fluid

The assumptions for the boundary-layer equations are valid only for high Reynolds number. For a power-law fluid the *Re* number is defined as follows

$$Re_\infty = \frac{\rho_\infty}{m}u_\infty^{2-n}L^n.$$

In the development of the momentum and energy equations (15) and (20), we obtain the nondimensional *Re* number as a function of the momentum thickness δ_2. Then,

$$Re_{\delta_2} = \frac{\rho_\delta}{m}u_\delta^{2-n}\delta_2^n. \quad (23)$$

This *Re* number satisfies the boundary-layer conditions as shown by Acrivos *et al.* [1]. For $n < 2$ the *Re* number increases with u_δ and the boundary layer exist for high *Re* number. For $n > 2$ the *Re* number decreases with u_δ and the boundary layer cannot exist beyond some value of u_∞.

Suction condition

Similarly to the Reynolds number the suction parameter at the infinity is defined by

$$\psi_\infty = \frac{\rho}{m}(-v_0)^{2-n}L^n.$$

This parameter was used by Spalding and Evans [9], Schlichting [6] and Truckenbrodt [10]. This parameter can be defined as the function of the momentum thickness δ_2 as follows:

$$\psi_{\delta_2} = \frac{\rho}{m}(-v_0)^{2-n}\delta_2^n.$$

Then,

$$\chi = [\psi_{\delta_2}Re_{\delta_2}^{1-n}]^{1/(2-n)} \quad (24)$$

and for $n = 1$ result $\chi = \psi_{\delta_2}$.

Truckenbrodt [10] studies the behaviour of this parameter for bidimensional and axisymmetric flow, whereas Spalding and Evans [9] present tables for this parameter in the similar solution.

The velocity profile

Approximate methods for the solution of the boundary-layer equations usually employ polynomial expressions for the velocity profile. The more these profiles satisfy a greater number of boundary conditions the more exact is the solution. The form of parameters used for the velocity profile are adjustable to accelerated or de-accelerated flow. Polynomials with fixed degree were used by some authors [6, 10]. From the analysis of Mangler and Wieghardt concerning the behaviour of polynomials for the integral solution Geropp [3] suggested a biparametric profile of variable degree. He concludes that with a fixed degree it happens that $u/u_\delta > 1$ and that in the neighbourhood of the stagnation point a polynomial of the 20th degree for the velocity profile is needed. In the neighbourhood of the separation point only a polynomial of the fourth degree is sufficient to fit the velocity profile. His results, when compared to the results of the exact solution given by Görtler [3], present excellent agreement. In our case introducing the slip velocity results,

$$\frac{u}{u_\delta} = 1-(1-\eta)^\xi(1-k+a_1\eta+a_2\eta^2+a_3\eta^3) \quad (25)$$

where

$$\eta = \frac{y}{\delta}$$

$$k = \frac{u_0}{u_\delta}.$$

This profile satisfies the boundary conditions at $y = 0(u = u_0)$ and $y = \delta(u = u_\delta)$.

The coefficients a_1, a_2 and a_3 are determined using the following defined form parameters [3, 11],

$$\gamma_{(x)} = -\left.\frac{\partial^2(u/u_\delta)}{\partial\eta^2}\right|_{\eta=0}$$

$$\Gamma = -\left.\frac{\partial^2(u/u_\delta)}{\partial(y/\delta_2)^2}\right|_{y=0} \quad (26)$$

$$\varepsilon_{(x)} = \left.\frac{\partial(u/u_\delta)}{\partial\eta}\right|_{\eta=0}$$

than,

$$a_1 = (1-k)\xi-\varepsilon$$

$$a_2 = \frac{\gamma}{2}-\xi\varepsilon+(1-k)\frac{\xi^2+\xi}{2} \quad (27)$$

Using the derivative of the compatibility condition equation (22), for $y = 0$,

$$v_0\left.\frac{\partial^2u}{\partial y^2}\right|_{y=0} = n\frac{m}{\rho}\left[(n-1)\left(\frac{\partial u}{\partial y}\right)^{n-2}\left(\frac{\partial^2u}{\partial y^2}\right)^2 + \left(\frac{\partial u}{\partial y}\right)^{n-1}\frac{\partial^3u}{\partial y^3}\right]_{y=0}$$

and the definition of Γ and the suction parameter χ results:

$$a_3 = \frac{\gamma}{6}\left[3\xi-(n-1)\frac{\gamma}{\varepsilon}+\frac{1}{n}\chi\varepsilon^{1-n}\left(\frac{\Gamma}{\gamma}\right)^{-n/2}\right] -\varepsilon\frac{\xi^2+\xi}{2}+(1-k)\frac{\xi^3+3\xi^2+2\xi}{6}. \quad (28)$$

These coefficients are functions of the parameters ξ, γ, ε and χ. The suction parameter χ appears in the coefficient a_3. Geropp [3] demonstrated that using the Hartree solution the variable exponent parameter ξ is a function of the parameter ε. The following expression was obtained by Geropp [3]:

$$\xi(x) = 7+1.7513\varepsilon-0.7026\varepsilon^2, \quad 0 < \varepsilon < 1$$

and (29)

$$\xi(x) = 8-0.0235\varepsilon+0.0722\varepsilon^2, \quad \varepsilon > 1.$$

In this way a triparametric velocity profile is obtained. For a Newtonian fluid ($n = 1$), no suction ($v_0 = 0$) and no slip velocity ($u_0 = 0$) the expressions of the coefficients a_1, a_2 and a_3 are identical to those derived by Geropp [3].

The drag and dissipation coefficients

From the usual defined drag coefficient c_f [equation (11)] and using the expression for the shear stress for a power low fluid the following nondimensional expressions are obtained:

$$c_f = 2\frac{\left[\frac{\partial(u/u_\delta)}{\partial(y/\delta_2)}\right]^n_{y=0}}{\frac{\rho_\delta}{m}u_\delta^{2-n}\delta_2^n}. \quad (30)$$

Usually α is defined by the following expression [10]

$$\alpha = \left.\frac{\partial(u/u_\delta)}{\partial(y/\delta_2)}\right|_{y=0} \quad (31)$$

Using equation (23) the value of c_f is given by

$$c_f = 2\frac{\alpha^n}{Re_{\delta_2}}. \quad (32)$$

Similarly from equation (16) and from the expression for the shear stress of a non-Newtonian fluid the following nondimensional expression for the dissipation coefficient C_D is obtained:

$$C_D = k\frac{\alpha^n}{Re_{\delta_2}}+\frac{1}{\frac{\rho_\delta}{m}u_\delta^{2-n}\delta_2^n} \times\int_0^{\delta/\delta_2}\left[\frac{\partial(u/u_\delta)}{\partial(y/\delta_2)}\right]^{n+1}\mathrm{d}(y/\delta_2). \quad (33)$$

Usually β is defined by the following expression [11]:

$$\beta = \int_0^{\delta/\delta_2}\left[\frac{\partial(u/u_\delta)}{\partial(y/\delta_2)}\right]^{n+1}\mathrm{d}(y/\delta_2). \quad (34)$$

Then

$$C_D = \frac{1}{Re_{\delta_2}}(k\alpha^n+\beta). \quad (35)$$

Numerical solution

The method of solution used was developed by Geropp [3, 7, 11] and can be applied for laminar boundary-layer flow with variable physical properties, adiabatic or not, and with pressure gradient. Our solution considers the problem of steady state, laminar and isothermal incompressible flow. The integral conditions of the momentum and mechanical energy equations and the compatibility conditions as well as the suction condition are solved simultaneously using the triparametric velocity profile given by equation (25).

Substituting the expressions of c_f and C_D from equations (32) and (33) in the momentum equation (15) and mechanical energy equation (20) results in:

$$\frac{\mathrm{d}\delta_2}{\mathrm{d}x}+\left(2+\frac{\delta_1}{\delta_2}\right)\frac{\delta_2}{u_\delta}\frac{\mathrm{d}u_\delta}{\mathrm{d}x}-\frac{\alpha^n}{Re_{\delta_2}}-(1-k)\frac{v_0}{u_\delta} = 0 \quad (36)$$

and

$$\frac{d\delta_3}{dx}+3\delta_3\frac{1}{u_\delta}\frac{du_\delta}{dx}-\frac{2}{Re_{\delta_2}}(k\alpha^n+\beta)-(1-k^2)\frac{v_0}{u_\delta}=0. \quad (37)$$

At this point new variables are defined [3]

$$Z_J = Re_{\delta_2}\delta_2 = \frac{\rho}{m}u_\delta^{2-n}\delta_2^{n+1}$$
$$Z_E = Re_{\delta_2}\delta_3 = \frac{\rho}{m}u_\delta^{2-n}\delta_2^n\delta_3 \quad (38)$$

Substituting equation (38) into equations (36) and (32) results in:

$$\frac{dZ_J}{dx}+G_JZ_J-F_J=0$$
$$\frac{dZ_E}{dx}+G_EZ_E-F_E=0. \quad (39)$$

Equations (39) are linear differential equations of the first order of variable coefficients, where

$$G_J = 4n\frac{1}{u_\delta}\frac{du_\delta}{dx}$$
$$F_J = (n+1)\alpha^n-[(n+1)H_{12}-n]Z_J\frac{1}{u_\delta}\frac{du_\delta}{dx} - (n+1)(1-k)\chi$$
$$G_E = (3n+1)\frac{1}{u_\delta}\frac{du_\delta}{dx} \quad (40)$$

and

$$F_E = 2(k\alpha^n+\beta)+nH_{32}(\alpha^n-Z_J)H_{12}\frac{1}{u_\delta}\frac{du_\delta}{dx} - \chi[n(1-k)H_{32}+1-k^2]$$

The compatibility condition, equation (22), is used simultaneously for the solution of these equations. Using the suction parameter, equation (24), and the following form parameter Γ

$$\Gamma = -\frac{\partial^2 u/u_\delta}{\partial(y/\delta_2)}\bigg|_{y=0} = \left(\frac{\delta_2}{\delta}\right)^2\gamma \quad (41)$$

the nondimensionless expression is obtained

$$\Gamma = \frac{1}{n\alpha^{n-1}}\left[(1-k^2)Z_J\frac{1}{u_\delta}\frac{du_\delta}{dx}+\alpha\chi\right] \quad (42)$$

with this expression the coefficients F_J and F_E are transformed to:

$$F_J = (n+1)\alpha^n-[(n+1)H_{12}-n]\frac{1}{1-k^2} \times[n\alpha^{n-1}\Gamma-\alpha\chi]-(n+1)(1-k)\chi \quad (43)$$

and

$$F_E = 2(k\alpha^n+\beta) + nH_{32}\left[\alpha^n-\frac{H_{12}}{1-k^2}(n\alpha^{n-1}\Gamma-\alpha\chi)\right] - \chi[n(1-k)H_{32}+1-k^2] \quad (44)$$

where

$$H_{12}=\frac{\delta_1}{\delta_2}$$
$$H_{32}\frac{\delta_3}{\delta_2}=\frac{Z_E}{Z_J}.$$

These are universal functions and are calculated independently from the specific problem using the triparametric velocity profile, equation (25). These coefficients are functions only of the form parameters H_{32} and Γ and the suction parameter χ.

The momentum and mechanical energy equations (39) are solved by the quadrature method according to Walz [11] considering small intervals of Δx. In this case it is possible to consider the average values of the form parameter $\bar{H}_{32}$ and $\bar{\Gamma}$ and the suction parameter $\bar{\chi}$ and consequently the coefficients $\bar{F}_J$ and $\bar{F}_E$ are considered constant. Thus

$$\bar{F}_J = F_J(\bar{H}_{32},\bar{\Gamma},\bar{\chi})$$
$$\bar{F}_E = F_E(\bar{H}_{32},\bar{\Gamma},\bar{\chi}).$$

Then for every step i and $i+1$ from equations (39) results in:

$$\frac{Z_{J_{i+1}}}{Z_{J_i}} = A_J+\frac{\bar{F}_J}{Z_{J_i}}B_J \quad (45)$$

and

$$\frac{Z_{E_{i+1}}}{Z_{E_i}} = A_E+\frac{\bar{F}_E}{Z_{E_i}}B_E$$

where

$$A_J = \left[\frac{u_{\delta_i}}{u_{\delta_{i+1}}}\right]^{4n}$$
$$A_E = \left[\frac{u_{\delta_i}}{u_{\delta_{i+1}}}\right]^{3n+1}$$
$$B_J = \frac{1}{u_{\delta_{i+1}}^{4n}}\int_{x_i}^{x_{i+1}}[u_\delta(x)]^{4n}dx \quad (46)$$

and

$$B_E = \frac{1}{u_{\delta_{i+1}}^{3n+1}}\int_{x_i}^{x_{i+1}}[u_\delta(x)]^{3n+1}dx.$$

The external velocity $u_\delta(x)$ is given and the convergence is assumed if for small enough interval $(x_{i+1}-x_i)$ the condition [11]

$$0.97 \leqslant \frac{u_{\delta_{i+1}}}{u_{\delta_i}} \leqslant 1.03$$

is satisfied.

The potential velocity

The pressure distribution or potential velocity is usually determined experimentally or from the potential theory. The potential velocity can be represented as a function of x in terms of a power series. Blasius solution needs a large number of terms in the series in the neighbourhood of the stagnation point. Hiemenz [3] demonstrated experimentally that Blasius solution is satisfied in the neighbourhood of the stagnation point but fails near the separation point. Loitsianskii

[4] shows that in the neighbourhood of the separation point the deviation of the theoretical and experimental results are of the order of 25%. The potential velocity for a circular cylinder is usually represented by a sinusoidal distribution corresponding to the velocity distribution of the potential flow. It is important to note that the potential flow theory does not predict boundary-layer separation and hence this is not a real potential velocity. From experimental results of the pressure distribution over a circular cylinder Hiemenz [3, 7] presented the following expression for the potential velocity.

$$u_\delta(x) = 7.151x - 0.04497x^3 - 0.00033x^5$$

valid for a circular cylinder of radius $R = 4.87$ cm and for

$$u_\infty = 19.2\ \mathrm{cm/s}$$
$$Re_\infty = 18\,500.$$

This expression satisfies the solution of the boundary-layer equation for high values of x whereas the series expression satisfies this solution only for small values of x. The above expression written in a dimensionless form, is given by

$$u^* = x^* - 0.006289x^* - 0.00004615x^{*5} \qquad (47)$$

where

$$u^* = \frac{u_\delta}{Ku_\infty}$$

$$x^* = \frac{x}{L}$$

$$L = 1\ \mathrm{cm}$$

or

$$u^* = x^* - 0.14914x^{*3} - 0.02582x^{*3} \qquad (48)$$

where

$$x^* = \frac{x}{R}.$$

This formal representation was introduced by Görtler [6] and used by Geropp [3], Smith and Clutter [8]. Since for $x^* \cong 7.0 (x^* = x/L)$ the results calculated from this expression agrees well with the experimental results and since the separation point occurs for $x^* < 7.0$ we can perfectly use this expression for the external velocity profile.

The suction parameter

The suction parameter χ defined in equation (24) is a function of v_0 and u_δ. Instead of the defined relation v_0/u_δ it is more convenient to define the "suction level" as the ratio of the Reynolds number for δ_2 and for Re at the infinity for it is independent of the particular conditions of the flow:

$$\frac{\psi_{\delta_2}}{\psi_\infty} = \frac{Re_{\delta_2}}{Re_\infty} = \left(\frac{\delta_2}{L}\right)^n.$$

Then substituting this expression and the defined thickness parameter $\delta_2 = Z_J/Re_{\delta_2}$ in equation (24) the following expression for the suction parameter is obtained:

$$\chi = \left[\frac{\psi_\infty}{Re_\infty^{(2n-1)/(n+1)}} \frac{1}{\left(\dfrac{Re_{\delta_2}}{Re_\infty^{1/(n+1)}}\right)^{2n-1}} \left(\frac{Z_J}{L}\right)^n\right]^{1/(2-n)} \qquad (49)$$

where

$$\nabla = \frac{\psi_\infty}{Re_\infty^{(2n-1)/(n+1)}}$$

is the "suction level".

The Reynolds number, Re_{δ_2}

From the defined Re_{δ_2} [equation (23)] and Re_∞ and the thickness parameter Z_J results from equation (38).

$$\frac{Re_{\delta_2}}{Re_\infty^{1/(n+1)}} = \left[\left(\frac{Z_J}{L}\right)^n \left(\frac{u_\delta}{u_\infty}\right)^{2-n}\right]^{1/(n+1)}. \qquad (50)$$

The momentum thickness δ_2

The momentum thickness δ_2 is determined from equation (38). Thus,

$$\frac{\delta_2}{L} Re_\infty^{1/(n+1)} = \left[\frac{Re_{\delta_2}}{Re_\infty^{1/(n+1)}} \left(\frac{u_\delta}{u_\infty}\right)^{n-2}\right]^{1/n}. \qquad (51)$$

The drag and the dissipation coefficients c_f *and* C_D

After some manipulations of equations (32) and (35) we get

$$c_f Re_\infty^{1/(n+1)} = \frac{2\alpha^n}{\dfrac{Re_{\delta_2}}{Re_\infty^{1/(n+1)}}} \qquad (52)$$

and

$$C_D Re_\infty^{1/(n+1)} = \frac{k\alpha^n + \beta}{\dfrac{Re_{\delta_2}}{Re_\infty^{1/(n+1)}}}. \qquad (53)$$

The wall shear stress τ_0

The wall shear stress τ_0 is determined from equations (11) and (52). Thus,

$$\frac{\tau_0 Re_\infty^{1/(n+1)}}{\rho u_\infty^2} = \frac{\alpha^n}{\dfrac{Re_{\delta_2}}{Re_\infty^{1/(n+1)}}} \left(\frac{u_\delta}{u_\infty}\right)^2. \qquad (54)$$

RESULTS

The effect of suction of a Newtonian and non-Newtonian fluid flow over a circular cylinder is first observed from the dislocation of the separation point of the boundary layer satisfying the condition of $\alpha = 0$. Table 1 shows the results for some values of the suction level ∇ varying from zero to 0.25 and some values of the slip parameter k varying from zero to 0.0288. For suction levels of 25% without slip ($k = 0$) or combined suction and slip parameter values the separation point is dislocated to $x^* > 7$ ($\theta = 82.39°$). For $x^* \geqslant 7.1$ ($\theta = 83.57°$) this solution fails because of the limitation of the potential velocity profile of equation (47). For the non-Newtonian fluid flow ($n = 1.2$) without suction ($\nabla = 0.0$) and without slip ($k = 0$) the separation point is

Table 1. Values for x_s^* and θ_s for the separation point

		∇				
	k	0.00	0.10	0.15	0.20	0.25
x^*	0.00	6.800	6.890	6.930	6.970	7.005
θ		80.036	81.095	81.566	82.037	82.449
x^*	0.01	6.845	6.930		7.005	7.045
θ		80.566	81.566		82.449	82.920
x^*	0.02	6.885	6.965		7.040	
θ		81.036	81.978		82.861	
x^*	0.025	6.905	6.985			
θ		81.767	82.213			
x^*	0.0288	6.950				
θ		81.801				

Table 2. Initial values for the parameters H_{32}, Γ and χ for $n = 1$

		∇				
	k	0.00	0.10	0.15	0.20	0.25
H_{32}		1.6253	1.6248	1.6245	1.6243	1.6240
Γ	0.0000	0.0854	0.0901	0.0924	0.0947	0.0969
χ		0.0	0.0282	0.0417	0.0546	0.0671
H_{32}		1.6252	1.6248		1.6243	1.6240
Γ	0.0100	0.0854	0.0900		0.0945	0.0969
χ		0.0	0.0282		0.0546	0.0671
H_{32}		1.6253	1.6249		1.6243	
Γ	0.0200	0.0853	0.0898		0.0945	
χ		0.0	0.0282		0.0546	
H_{32}		1.6255	1.6249			
Γ	0.0250	0.0852	0.0898			
$\chi\chi$		0.0	0.0282			
H_{32}		1.6256				
Γ	0.0288	0.0851				
χ		0.0				

Table 3. Values of the parameter H_{32}, Γ and χ for the separation point

		∇				
	k	0.00	0.10	0.15	0.20	0.25
H_{32}		1.5565	1.5541	1.5537	1.5532	1.5537
Γ	0.00	−0.1343	−0.1473	−0.1528	−0.1582	−0.1634
χ		0.0	0.0595	0.0886	0.1171	0.1451
H_{32}		1.5503	1.5479		1.5477	1.5474
Γ	0.01	−0.1481	−0.1620		−0.1712	−0.1768
χ		0.00	0.0608		0.1193	0.1479
H_{32}		1.5441	1.5420		1.5420	
Γ	0.20	−0.1651	−0.1757		−0.1855	
χ		0.00	0.0621		0.1216	
H_{32}		1.5406	1.5385			
Γ	0.025	−0.1711	−0.1842			
χ		0.00	0.0626			
H_{32}		1.3248				
Γ	0.0288	−0.1923				
χ		0.00				

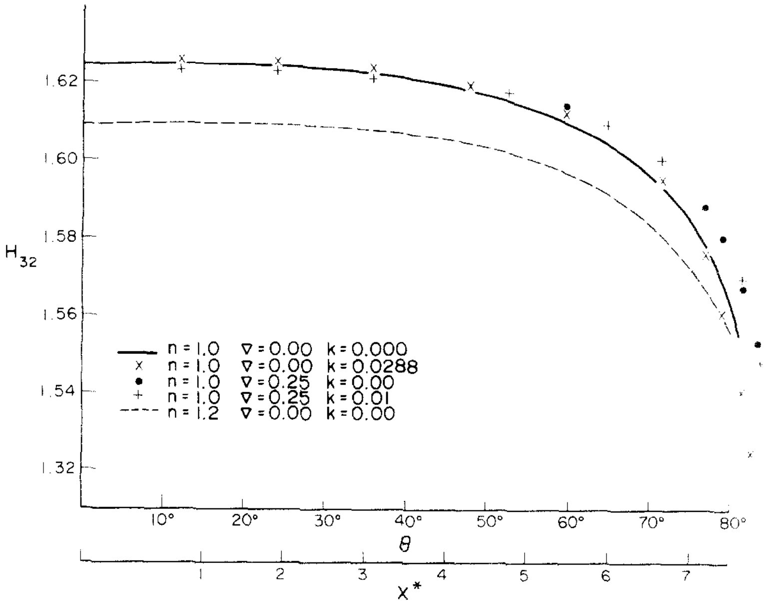

FIG. 2. The form parameter H_{32} vs x^*.

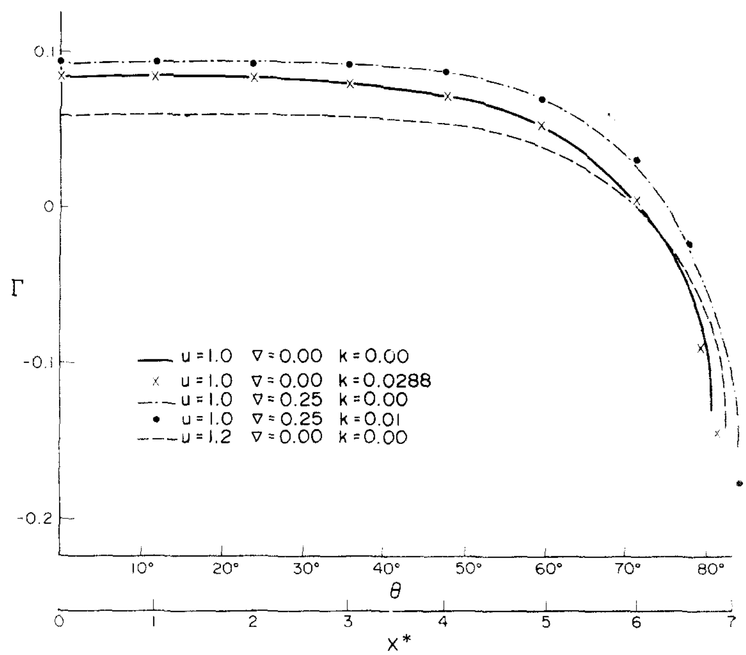

FIG. 3. The form parameter Γ vs x^*.

anticipated to the value of $x^* = 6.74$ ($\theta_s = 79.33°$). For Newtonian flow this value is given by $\theta_s = 80.036°$. This result was also obtained by Geropp [3], Smith and Clutter [8] and other authors. Applying suction to a Newtonian flow the separation point is dislocated 3% and with slip of 7% this pOint is dislocated by 3.6%.

Table 2 shows the initial values of the parameter H_{32}, Γ and χ for $n = 1$ at the stagnation point and Table 3 shows the final values of these parameters at the separation point. Figures 2 and 3 show the form parameter H_{32} and Γ as function of x^*. For a non-Newtonian fluid these values are smaller. For a suction level of 25% the values of these parameters are higher and still higher in the neighbourhood of the separation point.

The suction parameter as function of x^* is shown in Fig. 4 and the effect is increased for de-accelerated flow. For a Newtonian flow ($n = 1.0$) without slip ($k = 0$) and a suction level $\nabla = 0.1$ the suction parameter χ is 109% higher than the corresponding value at the stagnation point and for a suction level of $\nabla = 0.25$ this increment is of 116%. The effect of slip on the suction parameter is negligible. For $\nabla = 0.10$ and $k = 0.025$ the increment of χ from the stagnation point to the separation point is of 122% while for $\nabla = 0.25$ and $k = 0.01$ this increment is of 120%.

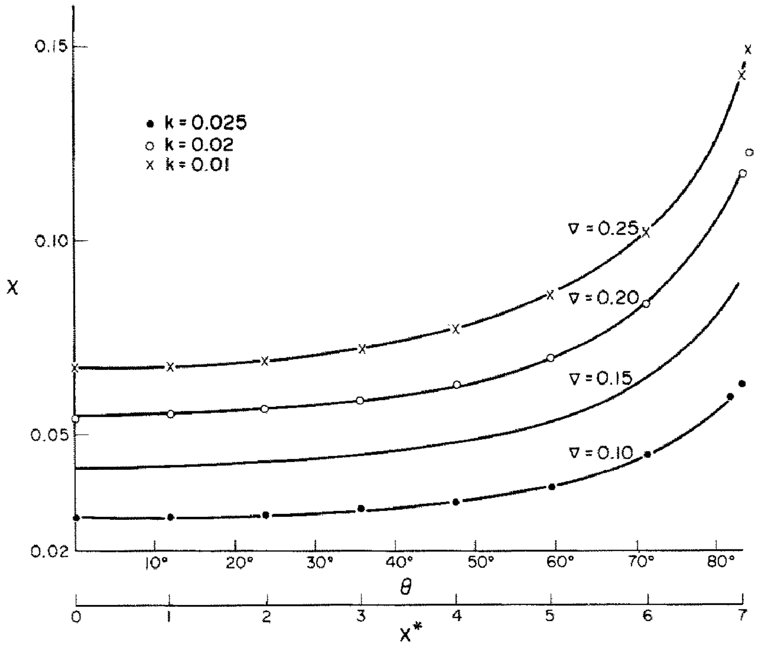

FIG. 4. The form parameter χ vs x^* for various suction levels V.

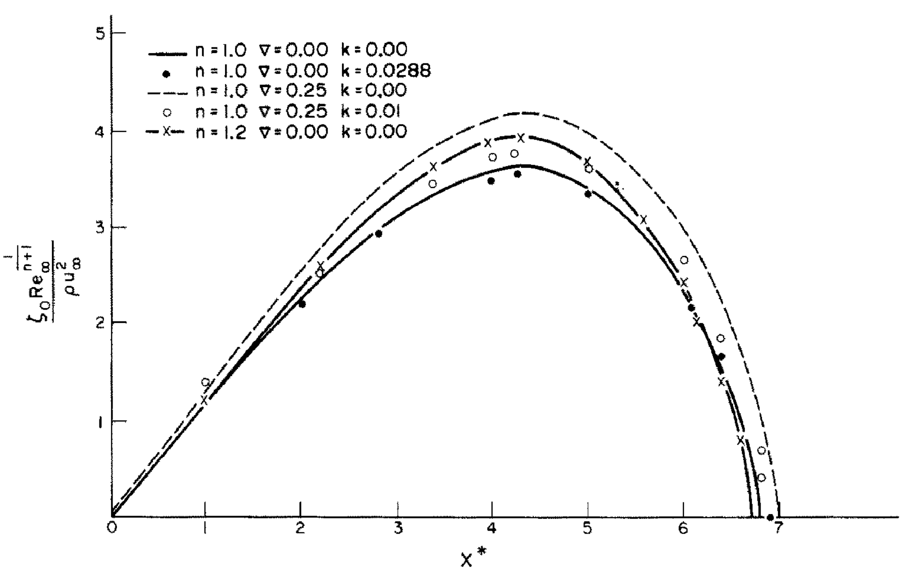

FIG. 5. Interfacial shear stress vs x^*.

Figure 5 shows the wall shear stress along the surface of the circular cylinder. For $n = 1$, $\mathrm{V} = 0$ and $k = 0$ the same results of Geropp [3] are obtained. Applying suction, τ_0 increases. At the point $x^* = 4.33$ ($\theta = 50.96°$) for $n = 1$, $\mathrm{V} = 0.25$ and $k = 0$ the values of τ_0 reaches the maximum value. Hence there is an increase of 15% when compared to the value of τ_0 without suction.

For a non-Newtonian fluid ($n = 1.2$) the wall shear stress is higher than for a Newtonian fluid for accelerated flow and lower in the neighbourhood of the separation point.

Figure 6 shows the potential velocity profile, the drag coefficient and the momentum thickness profile. For $n = 1.2$ the momentum thickness δ_2 is lower than for $n = 1$ in the neighbourhood of the stagnation point but increases rapidly and assumes the same profile as for a Newtonian flow in the neighbourhood of the separation point. Applying suction δ_2 decreases, particularly in the neighbourhood of the separation point where there is a decrease of 12.6% for $x_s^* = 6.8$. This means that the separation point is anticipated for a non-Newtonian fluid flow.

CONCLUSION

The suction effect on the boundary layer for a Newtonian and non-Newtonian fluid flow over a circular cylinder predicted by the present method of solution can be well observed accompanying the wall shear stress and the suction parameter along the

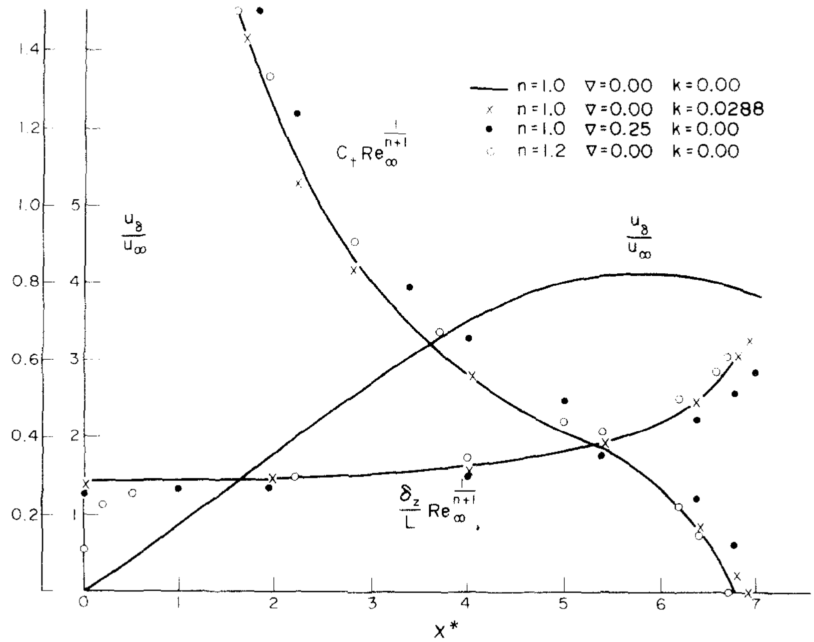

FIG. 6. The external velocity, the momentum thickness and the drag coefficient vs x*.

surface. By applying suction the separation point is dislocated. The separation point for a Newtonian fluid is 80.036° and for a non-Newtonian fluid ($n = 1.2$) without suction is reduced to 79.33° whereas applying suction of 25% the separation point dislocated to only 3%. The suction effect is more pronounced on the wall shear stress profile and mainly for the de-accelerated flow and higher suction levels. For suction level of 25% there is an increase of 15% in the wall shear stress corresponding to the maximum value of τ_0.

The suction parameter profile increases and is more pronounced in the neighbourhood of the separation point. Here an increase of 116% was observed applying suction of 25%. The slip velocity effect is negligible.

The results obtained by this method when compared to the results of the integral solution of Geropp and the exact solution of Görtler presents very close agreement.

REFERENCES

1. A. Acrivos, M. J. Shah and E. E. Petersen, Momentum and heat transfer in laminar boundary layer flows of non-Newtonian fluids past external surfaces, *A.I.Ch.E. Jl* **6**, 312 (1960).
2. G. D. Bizzel and J. C. Slattery, Non-Newtonian boundary-layer flow, *Chem. Engng Sci.* **17**, 777 (1962).
3. D. Geropp, Naherungstheorie für Kompressible laminare Grenzschichten mit zwei Formparameter fur das Geschwindigkeitsprofil, Dissertation, Karlsruhe (1963).
4. L. G. Loitzianskii, *Laminare Grenzschichten*. Akademie, Berlin (1967).
5. F. S. Neves, Efeitos viscosos em cilindros imersos em fluidos não-Newtonianos, Tese de M.Sc. COPPE (1972).
6. H. Schlichting, *Boundary Layer Theory*, 6th edn. McGraw-Hill, New York (1968).
7. M. Schmal, Eine Naherungslosung fur die Kondensation von laminar stromenden Dampf mit beliebigen Druckgradienten bei kleiner Mach-zahl und konstanten Stoffwerten, *Int. J. Heat Mass Transfer* **15**(5), 1137 (1972).
8. A. M. D. Smith and D. W. Clutter, Solution of the incompressible laminar boundary layer equations, *A.I.A.A. Jl* **9**, 2062 (1963).
9. D. B. Spalding and H. L. Evans, Mass transfer through laminar boundary layers, *Int. J. Heat Mass Transfer* **2**, 199 (1961).
10. E. Truckenbrodt, Ein einfaches Naherungsverfahren zum Berechnen der laminaren Reibungschicht mit Absaugung, *ForschHft. Ver. Dr. Ing.* **22**(5), 147 (1956).
11. A. Walz, *Boundary Layers of Flow and Temperature*. M.I.T., Cambridge, MA (1969).

EFFET DE L'ASPIRATION ET DE LA VITESSE DE GLISSEMENT D'UN FLUIDE NON NEWTONIEN S'ECOULANT AUTOUR D'UN CYLINDRE CIRCULAIRE

Résumé—On étudie l'effet de l'aspiration et de la vitesse de glissement sur la convection forcée d'un fluide newtonien ou en "loi puissance" sur un cylindre circulaire. On établit les équations de quantité de mouvement et d'énergie, les conditions de compatibilité et d'aspiration et on les résout à partir d'un polynome à trois paramètres variables pour le profil des vitesses. La méthode de Geropp et Walz est utilisée dans la recherche de la solution et le profil externe de vitesse de Hiemez–Görtler est appliqué pour l'écoulement autour d'un cylindre circulaire. L'effet de l'aspiration est observable en liaison avec la tension pariétale et le paramètre d'aspiration le long de la surface. Sans aspiration le point de décollement d'un écoulement de fluide non newtonien est avancé en comparaison d'un écoulement newtonien sur un cylindre circulaire. Avec aspiration, le point de décollement est déplacé. L'effet de l'aspiration est plus prononcé sur le profil de la tension pariétale et principalement pour les écoulements retardés et les très fortes aspirations. Le paramètre d'aspiration croît plus rapidement au voisinage du point de séparation. L'effet de la vitesse de glissement est négligeable.

DER EINFLUß VON ABSAUGUNG UND SCHLUPFGESCHWINDIGKEIT BEI DER UMSTRÖMUNG EINES KREISZYLINDERS MIT EINER NICHT-NEWTONSCHEN FLÜSSIGKEIT

Zusammenfassung—Der Einfluß von Absaugung und Schlupfgeschwindigkeit bei erzwungener Konvektion um einer Kreiszylinder wird untersucht. Der Kreiszylinder wird von einer Newtonschen Flüssigkeit und einem Fluid, dessen Fließverhalten mit dem Potenzansatz beschrieben werden kann (Ostwald-Flüssigkeit), umströmt. Die Impuls— und Energiegleichungen, die Kompatibilitäts— und Absaugbedingungen wurden hergeleitet und mittels eines Polynomansatzes für das Geschwindigkeitsprofil gelöst. Zur Lösung wird die Methose von Geropp und Walz benutzt und für die Umströmung eines Kreiszylinders wurde das äußere Geschwindigkeitsprofil von Hiemez-Görtler angewendet. Der Einfluß der Absaugung kann gut beobachtet werden, indem die Wandschubspannung und der "Absaug"-Parameter längs der Oberfläche verfolgt wird. Ohne Absaugung wird der Ablösepunkt einer nicht-Newtonschen Strömung früher erwartet, verlichen mit der Strömung einer Newtonschen Flüssigkeit um einen Kreiszylinder. Bei Absaugung wurde der Ablösepunkt verschoben. Der Einfluß der Absaugung ist stärker beim Wandschubspannungsprofil, insbesondere für die verzögerte Strömung und höhere Absaugraten. Der "Absauge"-Parameter steigt an der Nähe des Ablösepunktes stark an. Der Einfluß der Schlupfgeschwindigkeit ist vernachlässigbar.

ВЛИЯНИЕ ОТСОСА И СКОРОСТИ СКОЛЬЖЕНИЯ НА ОБТЕКАНИЕ КРУГОВОГО ЦИЛИНДРА НЕНЬЮТОНОВСКОЙ ЖИДКОСТЬЮ

Аннотация — Рассматривается влияние отсоса и скорости скольжения на обтекание кругового цилиндра неньютоновской жидкостью при вынужденной конвекции. Получены уравнения количества движения и энергии, а также условия отсоса и совместимости. Профиль скорости отыскивается в виде полинома с тремя параметрами. Для решения используется метод Джероппа–Вальца, при описании обтекания кругового цилиндра применяется внешний профиль скорости Химеца–Гёртлера. Влияние отсоса на характер обтекания проявляется в значениях касательного напряжения на стенке и параметра отсоса вдоль поверхности. Предполагается, что при отсутствии отсоса точка отрыва неньютоновской жидкости при обтекании цилиндра совпадает с точкой отрыва ньютоновской жидкости. При отсосе точка отрыва смещается. Влияние отсоса наиболее сильно сказывается на профиле касательного напряжения на стенке и в основном при заторможенном течении и более интенсивном отсосе. Вблизи точки отрыва параметр отсоса возрастает более резко. Влияние скорости скольжения пренебрежимо мало.